Control Engineering Practice 60 (2017) 7–17

Contents lists available at ScienceDirect

Control Engineering Practice

journal homepage: www.elsevier.com/locate/conengprac

Robust control for voltage and transient stability of power grids relying on wind power

Konstantin Schaab*, Jannik Hahn, Maksim Wolkov, Olaf Stursberg

Control and System Theory, Dept. Electrical Eng. and Computer Science, University of Kassel, Germany

ARTICLE INFO

Keywords:
Smart grids
Decentralized control
Robust control
Voltage control
Transient stability
Wind turbines

ABSTRACT

Common practice in stabilization of power grids is to refer to different stability categories (transient stability, voltage stability, rotor angle stability) and to address these by designing dedicated controllers separately based on models linearized around nominal operation points. Furthermore, the controllers of a generating unit contained in the grid are usually synthesized without considering other grid nodes. This work, in contrast, proposes a scheme for unified synthesis of controllers which conjunctively address rotor angle stability and voltage stability for grids containing synchronous generators as well as wind energy conversion systems based on doubly-fed induction generators. First, a procedure is proposed to describe the generating units by linear-parameter-varying (LPV) systems, in which fluctuations imposed by the grid or the wind are mapped into time-varying model parameters. For appropriate ranges of these parameters, decentralized robust controllers can be synthesized by semidefinite-programming, such that the power grid is stabilized for the considered fluctuations and disturbances. The effectiveness of the approach is demonstrated for a multi-bus benchmark system, where the grid oscillations are well damped and the LPV-controller stabilizes the grid after permanent changes.

1. Introduction

Ensuring stability has always been a main concern of power system operation, even more so since renewable energy intensifies fluctuations. To account for different measures of convergence for power grids, specific stability categories were introduced (Kundur et al., 2004): *frequency*, *rotor angle* and *voltage stability*. This work is concerned with the latter two categories, where rotor angle stability (also called transient stability) ensures that the synchronous generators (SG) remain synchronous after grid faults and that electromechanical oscillations are damped down in a reasonable time. Voltage stability is concerned with the restoration of a certain voltage level after the occurrence of a fault or for changing operating conditions. Though the two categories are physically interdependent, the respective standard controllers of power system components are often designed separately considering only one single control objective. Thus, unsatisfactory coordination between the controllers for one grid component can lead to performance degradation, or even to system failure (Gordon & Hill, 2008). Furthermore, the controllers of different grid components are usually designed independently, while assuming that all other components maintain their nominal behavior. However, the strong coupling throughout the grid renders this assumption questionable, e.g. in the case that synchronous generators (SG) and wind energy conversion systems (WECS) coexist - the focus of this paper. Typically, the local controller design for both systems are based on linearized models around operating points and the performance can degrade significantly with changing operating points. The transition of power grids to a more decentralized energy generation leads to more fluctuations. Hence, the design methods must be reconsidered to achieve sufficiently good robustness. The following literature review first surveys existing approaches for robust control of rotor angle and voltage for SG, and then discusses techniques for control of WECS. Combined control for transient stability and voltage control based on the technique of direct feedback linearization (DFL) is proposed in Gordon and Hill (2008). One controller is designed to control the rotor angle stability during a fault phase. In the post-fault period, a global controller activates the voltage regulator. Asymptotic stability for the whole grid is not proven and permanent faults / changes of operating points are not considered with respect to steady state accuracy of the voltage. In Fusco and Russo (2011), the voltage control loop restores the pre-fault voltage value, and an additional loop ensures synchronism. However, the system performance strongly depends on proper estimation of system parameters, and stability is not discussed. In Liu, Hu, and Song (2012), excitation control based on the DFL-technique is described, and asymptotic stability is ensured based on Lyapunov functions, but criteria such as robustness are not discussed. An overview for robust

* Corresponding author.
E-mail address: k.schaab@uni-kassel.de (K. Schaab).

http://dx.doi.org/10.1016/j.conengprac.2016.12.003
Received 7 June 2016; Received in revised form 6 December 2016; Accepted 7 December 2016
Available online 16 December 2016
0967-0661/

controllers designed for power systems is given in Fan (2009); Schaab and Stursberg (2015): One promising technique to ensure robust operation of the SG is the synthesis based on linear-parameter-varying(LPV) systems. The idea behind them is to transform the nonlinearities and the system variabilities into varying parameters of the LPV-system. Stabilizing the LPV-system for all parameters implies the stabilization of the original nonlinear system.

In Liu, Vittal, and Elia (2006a,b); Qiu, Vittal, and Khammash (2004), LPV techniques are used for robust control of SG and FACTS to enhance rotor angle stability by using sets of linearized models around several operating points. The success of this method to obtain LPV-models is highly dependent on a gridding process, and the original dynamics is not represented exactly. In He et al. (2006, 2009), an exact polytopic model of the SG is derived, including the grid equations of a small example of the grid. Stability is guaranteed as long as the parameters stay in the prescribed ranges, making this concept robust against sudden, and permanent changes. An application to larger grids does not appear possible for this method, since the LPV-model includes the algebraic equations of the grid, leading to very complicated models for larger grids. This drawback was addressed in Schaab and Stursberg (2015) and Schaab and Stursberg (2015), by deriving a decentralized and exact LPV-model of the SG in order to control the rotor angle. The changes within the grid and interconnections between the SGs of the power system are mapped in parameter ranges, making the resulting controller robust against the considered grid-changes. Using this approach for all grid nodes of a system assures grid-wide stability, as shown in Schaab and Stursberg (2015). While all discussed papers on techniques using LPV-models only address transient stability, none of them discusses the control of WECS as well.

However, other methods for WECS to improve rotor angle stability in case of system disturbances and to damp electromechanical oscillations exist. Since the electrical components react significantly faster than the mechanical ones (e.g. blade system, pitch system, and drive train) (Domínguez-García, Gomis-Bellmunt, Bianchi, & Sumper, 2012), they are solely discussed here. In Hughes, Anaya-Lara, Jenkins, and Strbac (2006), the control signal is added to the active power control loop of the standard DFIG converter controller to damp system oscillations. Likewise in Miao, Fan, Osborn, and Yuvarajan (2009) and Mishra, Mishra, Tripathy, Senroy, and Dong (2009), an additive signal on the standard control loops achieves a good damping using pole-placement. In all three cases, voltage control was not explicitely considered, but is included only by standard (reactive power) control loops. It is observed as a drawback that all controllers are based on linearization around operating points, i. e. robustness is not achieved for changing operating conditions. Again, LPV-based techniques may address robustness, and have already been used in the context of WECS. Most of the literature in this regard is concerned, however, with the damping of the mechanical oscillations to minimize fatigue loads, or with aerodynamic phenomena (e.g. Mohammadpour & Scherer, 2012). Some results are discussed nevertheless, to consider the existing LPV-models of WECS and their applicability to transient stability. In Wang and Weiss (2014), an approach to robust (grid) frequency control is presented, and detailed LPV-models of the mechanical and the electrical parts are derived. Through H_∞ controller design, a robustification against grid changes is introduced using an auxiliary disturbance input. However, only the electrical part of the WECS is considered for controller design, and a unified model of the electrical and mechanical equations is not presented. Instead, a switching mechanism is introduced to prevent the rotor speed from falling too low. Similarly in Muhando, Senjyu, Uehara, and Funabashi (2011), two LPV-models for the mechanical and electrical parts are presented, and one control loop each is designed to minimize fatigue loads and to damp the electrical torque fluctuations. To the best of the authors knowledge, a unified LPV-model of the WECS consisting of the electrical and mechanical parts for robust control of power grids including WECS after grid faults and for voltage control at the same time has not been presented so far.

The main contributions of this paper are (i.) to extend the technique for transient stabilization of a grid by SG as presented in Schaab and Stursberg (2015) to voltage control; for this reason a new exact LPV-model is derived, and a multiobjective, robust and decentralized LPV controller is synthesized to achieve transient stability, and to control the voltage; (ii.) an exact LPV-model of a WECS based on DFIG is derived such that it comprises the mechanical and electrical parts; (iii.) a method to damp grid-oscillations, to control the voltage and rotor angular velocity is proposed for the WECS. Using LPV-models and controller synthesis of the same type for all these aspects, this approach is unifying for grids comprising SG and WECS.

This paper is organized as follows: First, the standard nonlinear differential algebraic equations of a power system are presented in Section 2, comprising the equations of the SG, the DFIG-based WECS, and the grid. The derivation of the affine LPV-models for the SG and the WECS are presented in Section 3, followed by the description of the robust LPV-controller synthesis in Section 4. The resulting decentralized and robust controllers are illustrated by simulation for a multi-machine benchmark system in Section 5. Finally, the paper concludes with a discussion and a view on future work in Section 6.

2. Differential-algebraic model of the power grid

In this work, the two stability categories *transient stability* and *voltage stability* according to Kundur et al., 2004 are addressed. Thus, the power system model must include the electromechanical phenomena. The related equations are standard, and are typically formulated in dq-coordinates (indicated by the indices d and q throughout this chapter) and in *per units* (Kundur, 1994). For illustrative description this paper refers in different parts to a 9-bus-system as shown in Fig. 1. This system is taken from Anderson and Fouad (2003) and will be modified later by assuming that the generators (indicated by G_h, if connected to a bus with number h) are either realized as SG or as WECS.

Each of the dynamic components is modeled by first order DAE-equations of the type

$$\dot{x}(t) = f(x(t), y(t), u(t)), \tag{1}$$

$$0 = g(x(t), y(t), u(t)), \tag{2}$$

where $x \in \mathbb{R}^{n_d}$, $y \in \mathbb{R}^{n_a}$, and $u \in \mathbb{R}^m$, are the vectors of n_d differential variables, of n_a algebraic variables, and of m inputs.[1] The grid furthermore contains transformers T_h, the loads A, B, and C, and, of course, the connecting lines of the grid. Typically, in the context of the control objectives of this work, these components are modeled as constant impedances and can be encoded, together with the grid

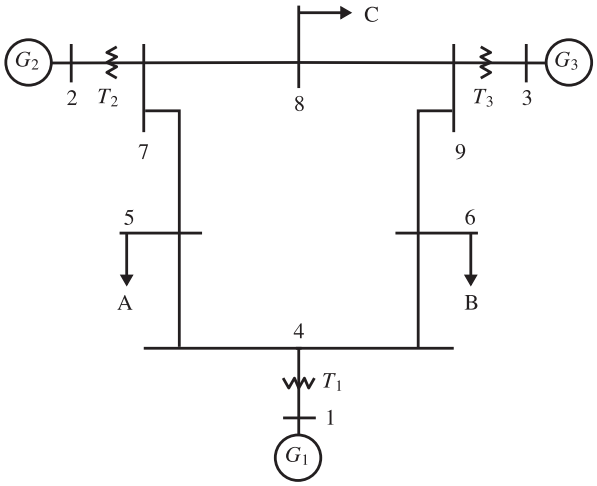

Fig. 1. Structure of the 9-bus-system.

connections, in the so called *admittance matrix* $\overline{Y} \in \mathbb{R}^{r}$ [2]. This matrix represents the grid structure, and can be used to calculate the four variables that characterize a bus: voltage v_h and its phasor φ_h, and the active and reactive powers (p_h, q_h). As some of these variables appear in the algebraic Eqs. (2), they establish the coupling of the grid nodes (shown in the subsequent sections). The vector $\overline{s} = [\overline{s}_1, \overline{s}_2, \ldots, \overline{s}_{n_s}]^T$ of complex powers $\overline{s}_h = p_h + jq_h$ for the bus h can be expressed by:

$$\overline{s} = \overline{V}\,\overline{Y}^*\overline{v}^* \tag{3}$$

if $\overline{V}$ is the voltage matrix and $\overline{v}^*$ the voltage vector. To simplify notation, the index h is in the following only used for the (algebraic) variables of the connecting bus h when occurring in the model equations of the SG and the WECS.

2.1. Model of the synchronous generator

Considering electromechanical phenomena, an SG can be modeled as a third order model with several algebraic variables and two inputs, as listed in Table 1. The three states are the rotor angle δ, the angular velocity ω, and the transient voltage e'_q. The dynamics of δ are specified by the difference between ω and the reference frequency ω_b, and the dynamics of ω by the difference between the two torques τ_m and τ_e. The respective equations are given as follows Kundur (1994); Milano (2010):

$$\dot{\delta} = \Omega_b(\omega - \omega_b), \tag{4}$$

$$\dot{\omega} = \frac{1}{2H}(\tau_m - \tau_e - D(\omega - \omega_b)), \tag{5}$$

$$\dot{e}'_q = \frac{1}{T'_{dO}}(-e'_q - (x_d - x'_d)i_d + v_f). \tag{6}$$

The two inputs of the system are τ_m and v_f. However, considering the control objectives of this work, τ_m can be considered as constant, as it is usually adjusted slowly compared to the dynamics of the states. Without going into detail, the remaining equations of the algebraic variables (Table 1) are defined by Milano (2010):

$$0 = \tau_e - (v_d + r_a i_d)i_d - (v_q + r_a i_q)i_q, \tag{7}$$

$$0 = v_q + r_a i_q - e'_q + x'_d i_d, \tag{8}$$

$$0 = v_d + r_a i_d - x_q i_q, \tag{9}$$

$$0 = v_d - v_h \sin(\delta - \varphi_h), \tag{10}$$

$$0 = v_q - v_h \cos(\delta - \varphi_h), \tag{11}$$

$$0 = p_h - v_d i_d - v_q i_q, \tag{12}$$

$$0 = q_h - v_q i_d + v_d i_q. \tag{13}$$

It is emphasized, that the SG is connected to the bus with the index h through the respective four variables in (10) to (13), which also occur in (3), and thus establish the coupling to the grid.

2.2. Models of the DFIG-based WECS

With the objective of including the same dynamic phenomena as for the SG, the WECS based on DFIG can be described as a third order model, including the dynamics of the drive train, the generator, and the converter Fernández, Jurado, and Saenz (2008). Assuming a rigid shaft, the remaining dynamics of the WECS, namely the turbine aerodynamics and the pitch system can be simplified to one power curve of the mechanical input $P_m(v_w, \beta, \omega_m)$, where v_w is the wind speed and β is the pitch angle Milano (2010). Due to the focus on transient and voltage stability through the generator, β is chosen to be constant. Without detailing the power curve equation, an example curve for a constant wind speed $v_w = 11.4\frac{m}{s}$ is depicted in Fig. 2. The mechanical torque can be calculated by $T_m = P_m/\omega_m$.

Table 1
Nomenclature for the SG.

States	
δ	Rotor angle
ω	Angular velocity
e'_q	Transient voltage
Inputs	
v_f	Field voltage
τ_m	Mechanical torque
Alg. variables	
i_d, i_q	Machine currents
v_d, v_q	Machine voltages
τ_e	Electrical torque
Machine parameters	
x_d, x_q	Synchronous reactances
x'_d	d-axis transient reactance
r_a	Armature resistance
Ω_b, ω_b	Base Synchronous/reference frequency
D	Damping coefficient
H	Inertia constant
T'_{dO}	d-axis open circuit transient time constant

Before introducing the model equations for the differential and algebraic variables in Table 2, some assumption concerning the DFIG are made: The grid side converter (GSC) is assumed to operate loss-less and synchronously with the grid. Thus, the active power of the GSC and of the rotor side converter (RSC) are equal, and the reactive power of the GSC is zero. Furthermore, due to the fact that the WECS is connected through the stator to the grid, which in turn is modeled by algebraic variables, the stator transients are neglected and $\dot{\psi}_{s,d} = 0$ and $\dot{\psi}_{s,q} = 0$ (Milano, 2010). The equations for the three states rotor speed ω_m and the rotor fluxes $\psi_{r,d}$ and $\psi_{r,q}$ are given as follows (Eremia & Shahidehpour, 2013):

$$\dot{\omega}_m = \frac{1}{2H_m}(T_m - T_{el}), \tag{14}$$

$$\dot{\psi}_{r,d} = v_{r,d} + r_r i_{r,d} + \omega_s s\psi_{r,q}, \tag{15}$$

$$\dot{\psi}_{r,q} = v_{r,q} + r_r i_{r,q} - \omega_s s\psi_{r,d}. \tag{16}$$

Eq. (14) shows that the difference between the mechanical and the electrical torque is the driving force of the rotor speed dynamics, while the inputs $v_{r,d}$ and $v_{r,q}$ affect the dynamics of the rotor fluxes. The remaining algebraic variables are determined by:

$$0 = T_{el} - x_\mu(i_{r,q}i_{s,d} - i_{r,d}i_{s,q}), \tag{17}$$

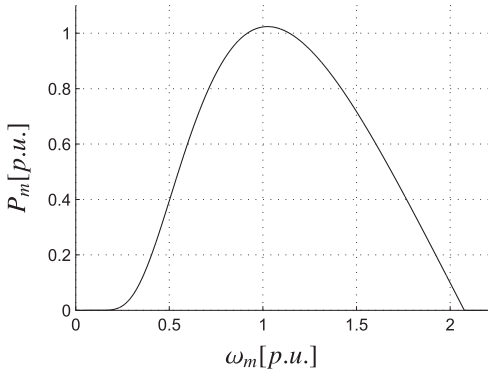

Fig. 2. $P_m(v_w, \beta, \omega_m)$ for a constant wind v_w=11.4 and a constant pitch angle $\beta = 0$.

[1] For brevity, the dependency of the variables on time t is omitted in the sequel.
[2] A bar $\bar{\bullet}$ and an asterisk $\bullet^*$ represent a phasor and the conjugate complex of a variable, respectively.

Table 2
Nomenclature for the WECS.

States	
ω_m	Rotor angular velocity
$\psi_{r,d}$, $\psi_{r,q}$	Rotor fluxes
Inputs	
$v_{r,d}$, $v_{r,q}$	Rotor voltages
Alg. variables	
$v_{s,d}$, $v_{s,q}$	Stator voltages
$i_{r,q}$, $i_{r,d}$	Rotor currents
$i_{s,d}$, $i_{s,q}$	Stator currents
s	Slip
T_m, T_{el}	Mechanical/electrical torque
Machine parameters	
x_r, x_s	Rotor/stator reactances
x_μ	magnetizing reactance
$x_{s,\mu}$, $x_{r,\mu}$	$x_{s,\mu} = x_s + x_\mu$, $x_{r,\mu} = x_r + x_\mu$
r_r, r_s	Rotor/stator resistances
H_m	Sum of turbine and rotor inertia
ω_s	Stator angular velocity

$$0 = -s + \left(\frac{\omega_s - \omega_m}{\omega_s}\right), \tag{18}$$

$$0 = v_{s,d} + r_s i_{s,d} + \omega_s \psi_{s,q}, \tag{19}$$

$$0 = v_{s,q} + r_s i_{s,q} - \omega_s \psi_{s,d}, \tag{20}$$

$$0 = \psi_{r,d} + (x_{r,\mu} i_{r,d} + x_\mu i_{s,d}), \tag{21}$$

$$0 = \psi_{r,q} + (x_{r,\mu} i_{r,q} + x_\mu i_{s,q}), \tag{22}$$

$$0 = \psi_{s,d} + (x_{s,\mu} i_{s,d} + x_\mu i_{r,d}), \tag{23}$$

$$0 = \psi_{s,q} + (x_{s,\mu} i_{s,q} + x_\mu i_{r,q}), \tag{24}$$

$$0 = v_{s,d} + v_h \sin\varphi_h, \tag{25}$$

$$0 = v_{s,q} - v_h \cos\varphi_h, \tag{26}$$

$$0 = p_h - v_{s,d} i_{s,d} - v_{s,q} i_{s,q} - v_{r,d} i_{r,d} - v_{r,q} i_{r,q}, \tag{27}$$

$$0 = q_h - v_{s,q} i_{s,d} + v_{s,d} i_{s,q}. \tag{28}$$

In these equations, the stator angular velocity ω_s is treated as a constant with the value one (synchronism of the GSC). The four bus variables of bus h contained in the last four equations represent the interface to the grid.

3. Transformation into LPV-models

The structure of an LPV-model is similar to the one of a linear model, but the matrices depend on time-varying parameters. The system dynamics is:

$$\dot{x}(t) = A(\theta(t))x(t) + B(\theta(t))u(t) \tag{29}$$

$$y(t) = C(\theta(t))x(t) + D(\theta(t))u(t) \tag{30}$$

where $x \in \mathbb{R}^{n_x}$ is the state vector, $y \in \mathbb{R}^{n_y}$ is the output vector, $u \in \mathbb{R}^{n_u}$ is the input vector, and $\theta(t) \in \mathbb{R}^p$ is the vector of time-varying parameters.

The objective now is to find LPV-models of the nonlinear DAE-systems of the SG and the WECS (Section 2). The resulting LPV-model should be an exact representation of these systems, i.e. only analytic transformations are used to preserve the original system behavior. Additional requirements for the system transformation are that the parameter vector $\theta(t)$ is computable from measurable quantities, and that the LPV-model is controllable.

In Tóth (2010) and Kwiatkowski et al. (2006), the idea of hiding the nonlinearities of ordinary differential equations (ODE) in the parameters to find a LPV-model description was presented. In Schaab and Stursberg (2015) and Schaab and Stursberg (2015), this idea was extended to DAE-systems. In the latter work, the original DAE-system was decomposed into sub-systems, and the coupling among the sub-systems was mapped into the parameters $\theta(t)$ through the algebraic variables. Thus, the parameters are dependent on states and algebraic variables.

In this work, these ideas for model transformation are reused and extended to the effects of the voltage (algebraic variable) at the point of connection. While the transformed model is not unique in general, the focus here is directed to the consistency of the local LPV-model to the original DAE-system and to controllability. Unlike to He et al. (2009), the modular system structure is preserved for decentralized control by not embedding the grid algebraic equations of (3) into the LPV-model. Thus, only the equations from Sections 2.1 and 2.2 are used for obtaining the respective LPV-models of the SG and WECS. For brevity, the time dependency of θ is omitted in the following.

3.1. LPV-model of a synchronous generator

In Schaab and Stursberg (2015), an LPV-model of the SG was already introduced for control of transient stability. In this work, the control objective is extended to voltage control, making a reformulation of the model necessary. The resulting LPV-model of type (29) is based on the state vector $x := [\delta, \Delta\omega, v_h]^T$, with $\Delta\omega = \omega - \omega_b$, and v_h is the controlled voltage at the connecting bus h. The input is defined as $u := v_f$.

While the dynamic model of the first state according to (4) is linear, the dynamics of x_2 and x_3 require transformations to obtain the LPV-form.

Starting from (5), τ_e is reformulated by inserting v_q from (8) and v_d from (9) into (7) to:

$$\tau_e = (x_q - x'_d) i_d i_q + e'_q i_q. \tag{31}$$

Using (31), x_2 can be written in LPV-form:

$$\dot{x}_2 = \frac{1}{2H}(\tau_m - (x_q - x'_d) i_d i_q - e'_q i_q - D(\omega - \omega_b)) = \frac{1}{2H}\theta_1 x_1 + \frac{-D}{2H} x_2 + \frac{-1}{2H}\theta_2 x_3 \tag{32}$$

where the parameter definitions are given below in (37). To get the LPV-form for the voltage, the algebraic variable v_h is first reformulated as a differential variable. Using the definition $v_h = \sqrt{v_d^2 + v_q^2}$, again inserting v_q and v_d, and setting r_a=0 leads to:

$$v_h \overset{r_a=0}{=} \sqrt{(x_q i_q)^2 + (e'_q - x'_d i_d)^2}\,. \tag{33}$$

As r_a typically has a very small value, the choice of 0 is justified for investigating transient stability (Gordon & Hill, 2008). To introduce v_h as the state x_3, it is differentiated with respect to time:

$$\dot{v}_h = \frac{1}{v_h}[x_q^2 i_q \dot{i_q} + (e'_q - x'_d i_d)(\dot{e'_q} - x'_d \dot{i_d})]. \tag{34}$$

Then, $\dot{e}'_q$ from (6) can be inserted. Thus, the dynamics of e'_q is subsumed in the dynamics of x_3, and e'_q is treated as component of the respective parameter, but not as a state. The LPV-description of $\dot{x}_3$ is then obtained to:

$$\dot{x}_3 = \frac{1}{x_3}(x_q^2 i_q \dot{i_q} - (e'_q - x'_d i_d) x'_d \dot{i_d}) + \frac{1}{x_3}(e'_q - x'_d i_d)\frac{1}{T'_{d0}}(-e'_q - (x_d - x'_d) i_d) + \frac{e'_q - x'_d i_d}{x_3} u = \theta_3 x_1 + \frac{1}{T'_{d0}}\theta_4 x_3 + \frac{1}{T'_{d0}}\theta_5 u, \tag{35}$$

with the parameters as defined below. Overall, the system can now be written as an LPV-model:

$$\dot{x} = \underbrace{\begin{pmatrix} 0 & \Omega_b & 0 \\ \frac{1}{2H}\theta_1 & \frac{-D}{2H} & \frac{-1}{2H}\theta_2 \\ \theta_3 & 0 & \frac{1}{T'_{do}}\theta_4 \end{pmatrix}}_{A(\theta)} x + \underbrace{\begin{pmatrix} 0 \\ 0 \\ \frac{1}{T'_{d0}}\theta_5 \end{pmatrix}}_{B(\theta)} u \tag{36}$$

where A and B are parameter-dependent, and $\theta(t)$ is composed of:

$$\theta_1 = (\tau_m - (x_q - x'_d) i_d i_q)\frac{1}{x_1},\ \theta_2 = e'_q i_q \cdot \frac{1}{x_3},$$
$$\theta_3 = \frac{x_q^2 i_q \dot{i_q} - (e'_q - x'_d i_d) x'_d \dot{i_d}}{x_3} \cdot \frac{1}{x_1},$$
$$\theta_4 = \frac{(e'_q - x'_d i_d)(-e'_q - (x_d - x'_d) i_d)}{x_3^2},$$
$$\theta_5 = \frac{e'_q - x'_d i_d}{x_3}. \tag{37}$$

Since the used transformations are analytic, the model (36), (37) exactly represents the models presented in Section 2.1. The two limitations $x_1 \neq 0$ and $x_3 \neq 0$ are not restrictive in practice, as $\delta = 0$ is not reached in the controlled case, and v_h=0 is not a relevant case for a controller (it represents a short-circuit).

The connection of the LPV-model to the grid is realized through the parameters, which in turn are governed by the currents i_d and i_q, their derivatives, and the voltage e_q'. The three variables can be calculated based on locally measurable quantities using the following equations (derived from the algebraic Eqs. (7) to (13):

$$i_d = \frac{p_h}{x_3}\sin(x_1 - \varphi_h) + \frac{q_h}{x_3}\cos(x_1 - \varphi_h),\ i_q = \frac{p_h}{x_3}\cos(x_1 - \varphi_h) - \frac{q_h}{x_3}\sin(x_1 - \varphi_h),\ e'_q = x'_d i_d + x_3 \cos(x_1 - \varphi_h). \tag{38}$$

The derivatives $\dot{i_q}$ and $\dot{i_d}$ can be estimated based on these equations.

3.2. LPV-model of a DFIG-based WECS

In this work, the controller objectives for the WECS concerning the grid stability are the same as for the SG, i.e. transient stability and control of voltage v_h at the connecting bus h. However, to assure the point of operation according to the power curve (see Section 2.2), the angular velocity ω_m is controlled as well. While ω_m is already formulated as a state in the original nonlinear model, a description of v_h in form of a differential equation has to be found. The resulting state vector can then be defined as $x := [\omega_m, \psi_{r,d}, \psi_{r,q}, v_h]^T$, and the input vector as $u := [v_{r,d}, v_{r,q}]^T$. Due to the fact that all state equations in Section 2.2 are nonlinear, the derivations of the LPV descriptions of each state are reported now.

The equation for x_1 in (14), is first expanded by $x_2 - x_2$ to avoid a zero-row for the subsequent choice for the first parameter in case of $T_m = T_{el}$. The controllability requirement can now be met with:

$$\dot{x}_1 = \frac{1}{2H_m}(T_m - T_{el}) + x_2 - x_2 = \theta_1 x_1 + x_2 \tag{39}$$

with the definition of θ_1 given below in (44).

To obtain the LPV-model for x_2, the stator frequency is assumed to be close to 1 p.u. (i.e. $\omega_s = 1$), and the slip simplifies to $s = (1 - \omega_m)$. Then, solving (21) for $i_{r,d}$ and inserting the latter into (15) leads to:

$$\dot{x}_2 = ((1 - x_1)x_3 - \frac{r_r x_\mu}{x_{r,\mu}} i_{s,d}) - \frac{r_r}{x_{r,\mu}} x_2 + u_1 = \theta_2 x_1 + \frac{-r_r}{x_{r,\mu}} x_2 + u_1. \tag{40}$$

The definition of the parameter θ_2 is described in (44). The derivation of the LPV-form for x_3 follows the same pattern using (22) and (16). To reformulate the algebraic variable v_h as a state x_4, the derivative of $v_h = \sqrt{v_{s,d}^2 + v_{s,q}^2}$ with respect to time leads to:

$$\dot{v}_h = (\dot{v}_{s,d} \cdot v_{s,d} + \dot{v}_{s,q} \cdot v_{s,q})\frac{1}{v_h}. \tag{41}$$

To ensure controllability, the equation is expanded by $x_2 - x_2 + x_3 - x_3$, and the LPV description for x_4 is:

$$\dot{x}_4 = x_2 - x_2 + x_3 - x_3 + \frac{\dot{v}_{s,d} v_{s,d} + \dot{v}_{s,q} v_{s,q}}{x_4} = x_2 + x_3 + \theta_4 x_4 \tag{42}$$

where θ_4 is defined below in (44). The LPV-model of the DFIG-based WECS can now be summed up to:

$$\dot{x} = \underbrace{\begin{bmatrix} \theta_1 & 1 & 0 & 0 \\ \theta_2 & \frac{-r_r}{x_{r,\mu}} & 0 & 0 \\ 0 & 0 & \frac{-r_r}{x_{r,\mu}} & \theta_3 \\ 0 & 1 & 1 & \theta_4 \end{bmatrix}}_{A(\theta)} x + \underbrace{\begin{bmatrix} 0 & 0 \\ 1 & 0 \\ 0 & 1 \\ 0 & 0 \end{bmatrix}}_{B} u \tag{43}$$

with the four parameters:

$$\theta_1 = \left(\frac{T_m - T_{el}}{2H_m} - x_2\right)\frac{1}{x_1},\ \theta_2 = \left((1 - x_1)x_3 - \frac{r_r x_\mu}{x_{r,\mu}} i_{s,d}\right)\frac{1}{x_1},$$
$$\theta_3 = \left((x_1 - 1)x_2 - \frac{r_r x_\mu}{x_{r,\mu}} i_{s,q}\right)\frac{1}{x_4},\ \theta_4 = \left(\frac{\dot{v}_{s,d} v_{s,d} + \dot{v}_{s,q} v_{s,q}}{x_4} - x_2 - x_3\right)\frac{1}{x_4}. \tag{44}$$

The LPV-model represents the nonlinear dynamics exactly if $x_1 \neq 0$ and $x_4 \neq 0$. Since x_1 corresponds to the rotor speed ω_m and x_4 to the voltage v_h, the value 0 refers to conditions for both variables (standstill and short-circuit), in which an operation of the WECS is not feasible and which are not within the relevant operating range for control. Thus, the applicability of the model is not compromised.

Furthermore, the connection to the grid is realized through the parameters, and they are in turn influenced by the stator currents $i_{s,d}$ and $i_{s,q}$, the stator voltages $v_{s,d}$ and $v_{s,q}$, and their derivatives $\dot{v}_{s,d}$ and $\dot{v}_{s,q}$. In contrast to the SG, the mechanical torque of the WECS T_m, can not be assumed as constant. It is influenced by the power curve, i.e. it is a function of the wind speed v_w and ω_m. However, due to the fact that T_m affects the parameter θ_1, the variation of the wind can be considered in the model. Thus, by using the parameter ranges for variations of θ in the subsequent controller synthesis, the controller can be designed robustly for variations of the grid and the wind. In difference to Muhando et al. (2011) and Wang and Weiss (2014), the model of the DFIG and the drive train are integrated into one model.

4. LPV controller synthesis

In this section, the technique for controller synthesis for the local controllers of the LPV-subsystems is presented. In contrast to the results presented in Schaab and Stursberg (2015), the input matrix B of the LPV-model for the SG is parameter dependent (see (36)). For a better distinction, the parameters affecting the matrix A are indexed with A and those affecting B are indexed with B. The objective of the synthesis technique presented here is to find an LPV state-feedback controller $K(\theta_A)$ which is scheduled by θ_A and is robust against changes of θ_B. The state-matrix of the closed-loop system is written as:

$$A_{cl}(\theta_A, \theta_B) = A(\theta_A) + B(\theta_B)K(\theta_A). \tag{45}$$

First, it is explained how the presented closed-loop matrix can be reformulated into polytopic form. Then, the synthesis technique is presented.

4.1. Polytopic system-description

An *affine* description of any parameter-dependent matrix $A(\theta_A)$ is given according to:

$$A(\theta_A) = \widetilde{A}_0 + \sum_{j=1}^{p} \theta_{A,j} \cdot \widetilde{A}_j, \tag{46}$$

with parameter bounds $\theta_{A,j} \in [\underline{\theta}_{A,j}, \overline{\theta}_{A,j}]$. Within these bounds, $A(\theta_A)$

varies within a convex hull $Co\{A_i: i = 1,\ldots,n_v\}$ with the vertices $A_i \in \mathbb{R}^{n_x \times n_x}$ Apkarian, Gahinet, and Becker (1995). The vertices A_i are defined by all combinations of the parameter bounds. The polytopic description of $A(\theta_A)$ can now be defined by its polytope $\mathcal{A}$:

$$A(\theta_A) \in \mathcal{A} := \left\{ \sum_{i=1}^{n_v} \alpha_i \cdot A_i : \sum_{i=1}^{n_v} \alpha_i = 1,\ \alpha_i \geq 0 \right\}. \tag{47}$$

Furthermore, the product of two matrix polytopes can again be described by a polytope, where the vertices of the convex hull are obtained by the combined products of the vertices of the polytopes (Bünger, 2014). By assuming that the three matrices $A(\theta_A)$, $B(\theta_B)$, and $K(\theta_A)$ of the closed loop system are affine in their parameter vectors, by using the polytopic matrix descriptions and the product of polytopes, the matrix $A_{cl}(\theta_A, \theta_B)$ in (45) can now be reformulated as a matrix polytope as well (Bünger, 2014):

$$\mathcal{A}_{cl} = \sum_{i=1}^{n_v} \alpha_i A_i + \sum_{j=1}^{n_b} \alpha_j B_j \sum_{i=1}^{n_v} \alpha_i K_i, \tag{48}$$

where the vertices of the convex hull $A_{cl,p}$ can be calculated by:

$$A_{cl,p} = A_i + B_j \cdot K_i \ \forall\ i = 1,\ldots,n_v,\ j = 1,\ldots,n_b \tag{49}$$

with $p \in \{1,\ldots,n_p\}$, and $n_p = n_v \cdot n_b$.

While the synthesis presented in the subsequent parts is carried out offline, the controller $K(\theta_A)$ needs to be scheduled online based on the measured (or calculated) parameter vector $\theta_A(t)$. Due to the fact that the controller is synthesized in terms of its polytopic description K_i, $\alpha_i(t)$ from (48) has to be retrieved from $\theta_A(t)$ first. A technique to formulate $\alpha_i(t)$ explicitely as a function $\alpha_i(t) = h(\theta_A(t))$ is described in Warren (1996). With known $\alpha_i(t)$, $K(\theta_A(t))$ can be calculated from its polytopic description, making the online computation of the control input $u(t) = K(\theta_A(t))x(t)$ a simple task.

4.2. Quadratic stability

If the parameter limits for θ_A and θ_B of the affine system are known, the state matrix of the closed-loop system can be described as (48) with the vertices (49). Starting from that, linear matrix inequalities (LMI) can be formulated, which ensure stability of the system for all parameter trajectories $\theta_A(t) \in [\underline{\theta_A}, \overline{\theta_A}]$ and $\theta_B(t) \in [\underline{\theta_B}, \overline{\theta_B}]$ under the condition that the LMIs are solved for each vertex of the polytope $A_{cl,p}$, $p \in \{1,\ldots,n_p\}$. Referring to the more general term *polytopic linear differential inclusions* (PLDI), Boyd, El Ghaoui, Feron, and Balakrishnan (1994) shows that *quadratic stability* is guaranteed for a PLDI if a symmetric matrix X can be found that satisfies:

$$[A_{cl,p}X + XA_{cl,p}^T] < 0,\ \forall\ p = 1,\ldots,n_p, \quad X > 0. \tag{50}$$

This formulation was used in Boyd et al. (1994) to design constant state feedback controllers. In Rotondo et al. (2013), the polytopic description presented in (49) is used to synthesize an LPV state-feedback controller that is robust against parameter changes in $\theta_B(t)$ for all $\theta_B(t) \in [\underline{\theta_B}, \overline{\theta_B}]$. Using the previous LMI formulation for quadratic stability, $A_{cl,p}$ from (49), and the auxiliary variables $Y_i = K_i X$, the robust controller can be retrieved by solving the following LMIs (Rotondo et al., 2013):

$$A_i X + X A_i^T + B_j Y_i + Y_i^T B_j^T < 0,\ \forall\ i = 1,\ldots,n_v,\ j = 1,\ldots,n_b, \quad X > 0. \tag{51}$$

The auxiliary variables Y_i are introduced to obtain (51) in linear form. The combination with H_∞-design and pole-placement constraints can be easily achieved by solving the corresponding LMIs together with the same matrix X (Chilali & Gahinet, 1996).

4.3. Pole-placement

By placing the poles of a closed-loop system in a specified region, the so-called $\mathfrak{D}$-*stability* can be established (Chilali & Gahinet, 1996). For brevity, only the LMIs for placing the poles in the left half-plane and within a conic sector are covered in the following.

By placing the poles $z \in \mathbb{C}$ of the closed-loop system according to bound $Re(z) < -\beta$, $\beta > 0$, a lower bound of the speed of convergence can be established and is enforced by the LMIs:

$$A_{cl,p}X + XA_{cl,p}^T + 2\beta X < 0,\ \forall\ p = 1,\ldots,n_p, \quad X > 0. \tag{52}$$

A deceleration of the system behavior (e.g. for numeric reasons) can be achieved by bounding the real parts of the poles to the right $Re(z) > -\beta$, by using (52) with ">" instead of "<" in the first inequality.

Considering transient stability, damping should be introduced into the power system dynamics. For this purpose, the admissible region for the poles is further restricted to a conic sector, using an angle ϕ between the real-axis and a line in the origin. The corresponding matrix inequalities to be solved are Chilali and Gahinet (1996):

$$\begin{bmatrix} \sin(\phi)(T_1) & \cos(\phi)(T_2) \\ -\cos(\phi)(T_2) & \sin(\phi)(T_1) \end{bmatrix} < 0,\ \forall\ p = 1,\ldots,n_p, \quad X > 0, \tag{53}$$

where T_1 and T_2 are defined as $T_1 := A_{cl,p}X + XA_{cl,p}^T$ and $T_2 := A_{cl,p}X - XA_{cl,p}^T$.

4.4. H_∞ performance

For the H_∞-controller design used in the context of this work, the LPV-system (29) has to be extended by exogenous inputs $w \in \mathbb{R}^{n_w}$ (e.g. disturbances) and by additional outputs $z \in \mathbb{R}^{n_z}$. Here, n_w and n_z denote the numbers of the exogenous inputs and outputs (Apkarian et al., 1995), leading to:

$$\dot{x}(t) = A(\theta_A)x(t) + B(\theta_B)u(t) + B_\infty w(t),\ z(t) = C_\infty x(t). \tag{54}$$

For the closed loop transfer function from w to z denoted by $G_{zw}(s)$, the quadratic H_∞-performance $\| G_{zw}(s) \|_\infty < \gamma$ is enforced by the following matrix inequalities (Apkarian et al., 1995):

$$\begin{bmatrix} A_{cl,p}X + XA_{cl,p}^T & B_{cl} & XC_{cl}^T \\ B_{cl}^T & -\gamma I & D_{cl}^T \\ C_{cl}X & D_{cl} & -\gamma I \end{bmatrix} < 0,\ \forall\ p = 1,\ldots,n_p, \quad X > 0, \tag{55}$$

with $B_{cl} = B_\infty$, $C_{cl} = C_\infty$, and $D_{cl} = 0$. These LMIs include the formulations for quadratic stability (Section 4.2).

4.5. Global stability

In Section 3, LPV-models (29) were derived for the SG and the WECS. Assuming that for all generating units of a grid the parameter ranges can be determined conservatively, then all relevant variations of the grid variables and fluctuations of the wind for the WECS are covered, and the presented controller technique can be used. The controller for a single SG or WECS is synthesized by solving the following semi-definite program:

$$\min_{K_i, X} \quad \gamma s.\ t.\ :(52),\ (53),\ \text{and}\ (55). \tag{56}$$

and the closed matrix $A_{cl,p}$ as described in (49). If for all sub-systems a feasible solution of this semi-definite problem exists, then the decentralized control with the robust local controllers $u(t) = K(\theta_A(t))x(t)$ implies the stabilization of the complete grid model. A sketch of the proof of this implication is contained in Schaab and Stursberg (2015).

5. Simulation results

The effectiveness of the proposed technique is demonstrated for the benchmark 9-bus-system introduced in Section 2.

To simulate the controllers for the SG and WECS, two variants of

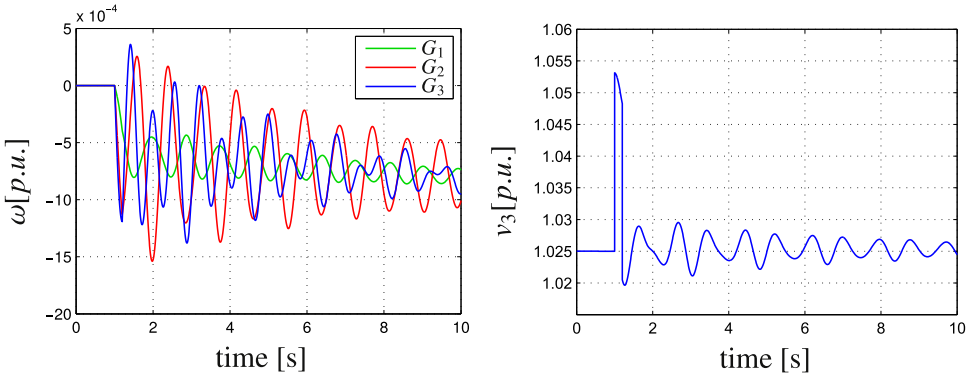

Fig. 3. Simulation of the SGs without control, scenario 1.

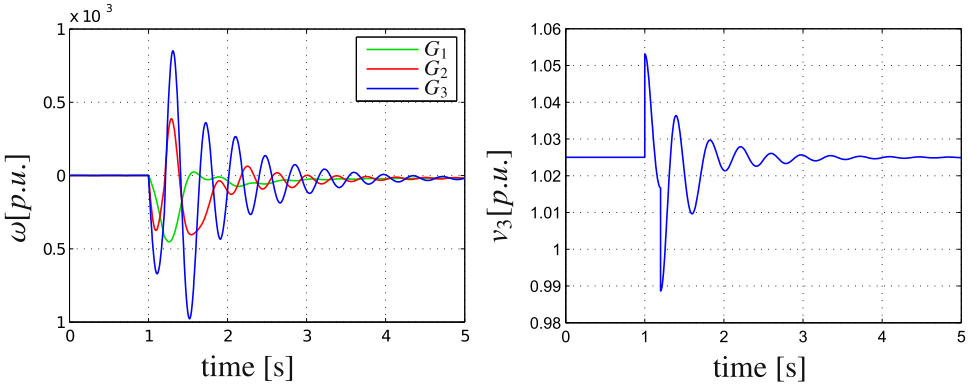

Fig. 4. Simulation of the SGs with standard control, scenario 1.

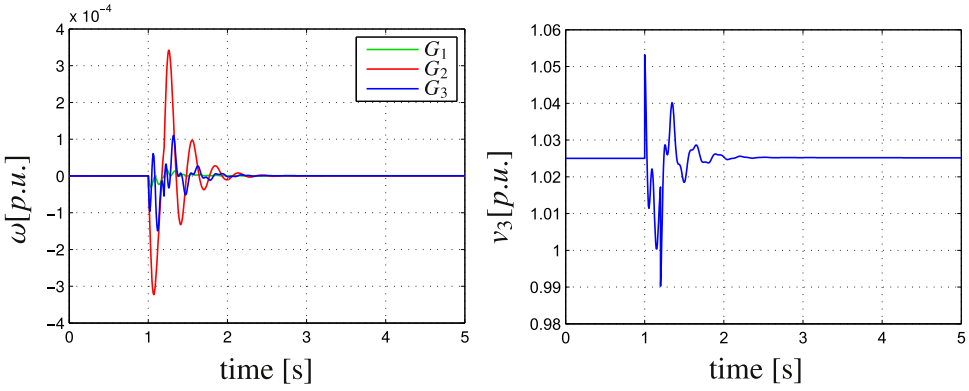

Fig. 5. Simulation of the SGs with LPV control, scenario 1.

this system are used: In the first variant, discussed in Section 5.1, all three generators are modeled as SG. While the control of G_3 addresses voltage control of v_3 at bus 3 and transient stability, the control of the G_1 and G_2 aims only at transient stability.[3] In the second variant of the benchmark system, discussed in Section 5.2, G_3 is replaced by the WECS W_3, and it is controlled by an LPV-controller. Due to the different source of energy, the rotor angle velocity ω_m of the WECS is controlled to influence the power extracted from the wind.

In order to obtain steady-state accuracy, integrating behavior is introduced for control of the voltage v_3 for both variants (i.e. x_3 of the SG G_3 and x_4 of the WECS W_3), and additionally for $x_1 = \omega_m$ of W_3. To work with similar shares of injected powers, the three generating units of the 9-bus-system are initialized to the three similar active powers $p_1 = 0.875\ p.u.$, $p_2 = 1\ p.u.$, and $p_3 = 0.9\ p.u.$ (on a 100 MVA base). The simulation scenarios are chosen to show that the presented LPV-controller (i) introduces good damping of oscillations after grid faults and (ii) is robust against permanent grid changes. In the case of the WECS, it is also shown that normal operation, i.e. changes of wind speed, can be handled as well. Robustness against the considered fluctuations of the operating conditions is ensured by the choice of large parameter ranges. The ranges are determined by iterating between simulation and controller synthesis, until a good performance is reached and the parameter ranges are not left during the simulation of the selected faults.

5.1. Control of the generator

Two scenarios are used to show transient stability and voltage control for the SG G_3. For scenario 1, at t=1 s the line admittance between the buses 5 and 7 is doubled for the duration $\Delta t = 0.2\ s$, i.e. the

[3] For the given grid, voltage control of G_1 and G_2 would require additional droop control, which is not covered here for space reasons.

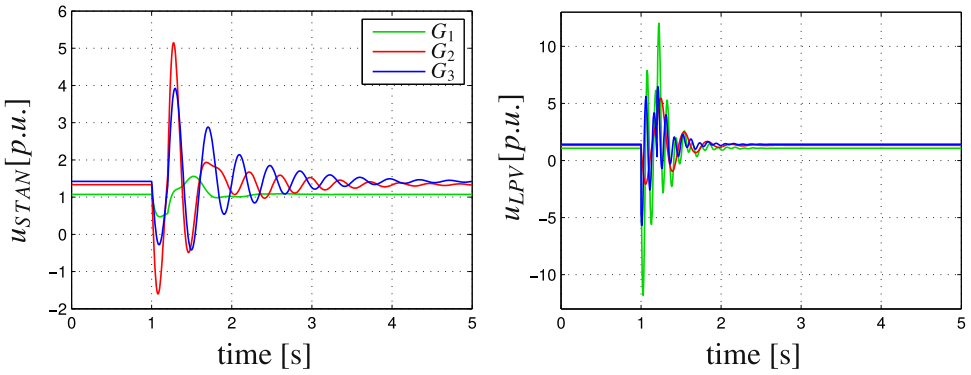

Fig. 6. Simulation results for the inputs of the SGs, scenario 1.

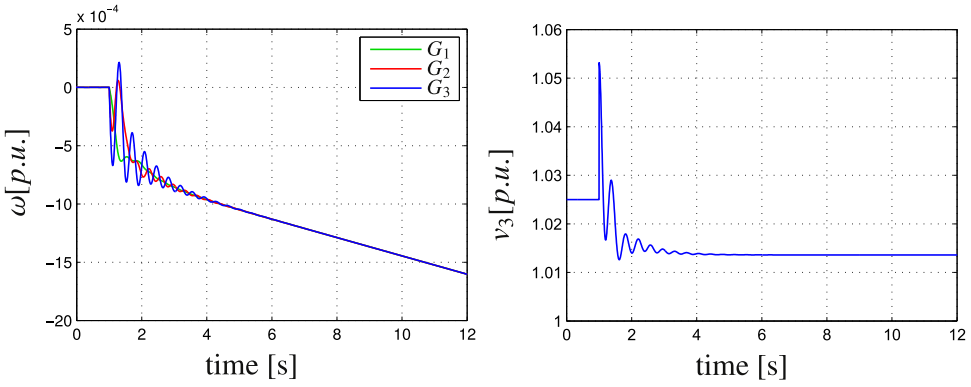

Fig. 7. Simulation of the SGs with standard control, scenario 2.

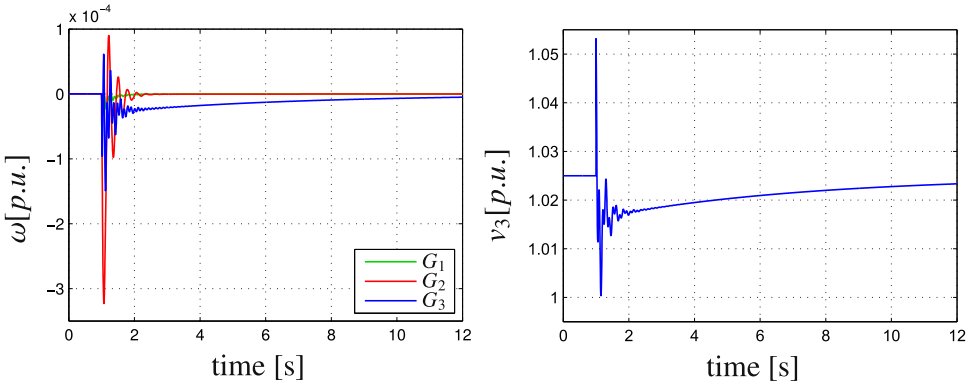

Fig. 8. Simulation of the SGs with LPV control, scenario 2.

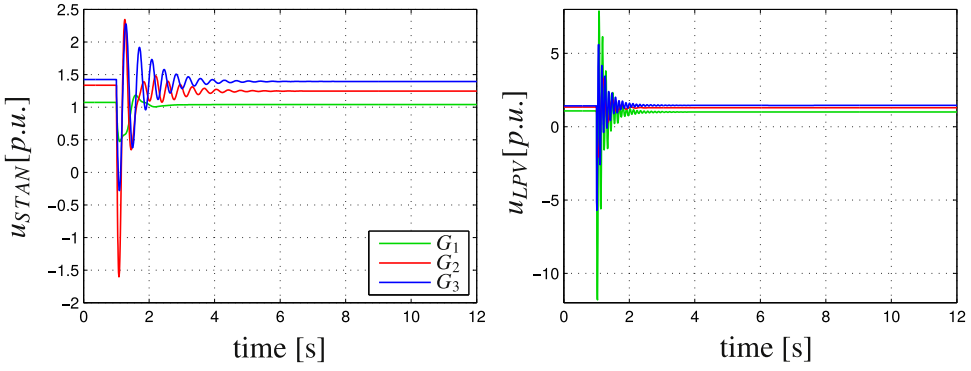

Fig. 9. Simulation results for the inputs of the SGs, scenario 2.

admittance matrix $\overline{Y}$ from Eq. (3) is changed. In scenario 2, the same line is switched at t=1 s and remains in this condition, changing the grid permanently.

First, scenario 1 is simulated without control, and Fig. 3 shows that the angular velocities ω of the three SGs begin to oscillate after the disturbance and drift away from the steady state. The hardly damped

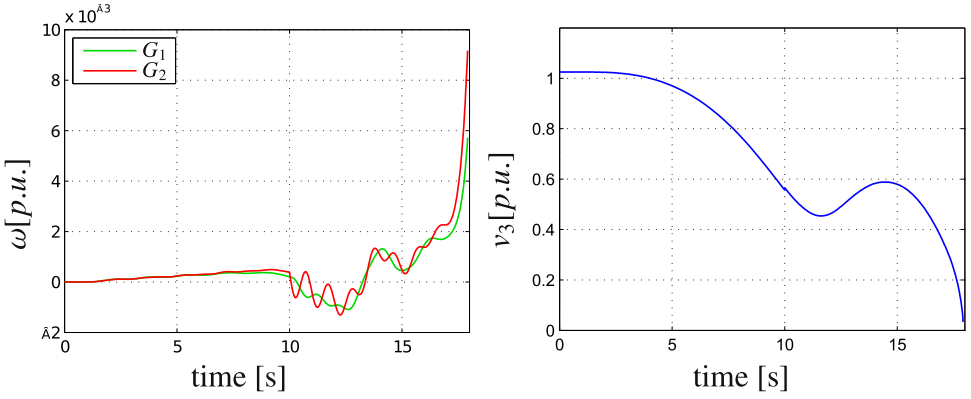

Fig. 10. Simulation of the SGs and WECS without control, scenario 3.

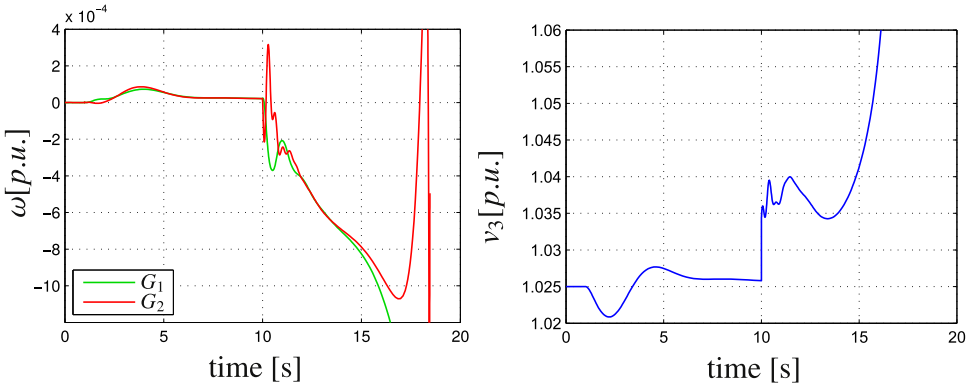

Fig. 11. Simulation of the SGs and WECS with standard control, scenario 3.

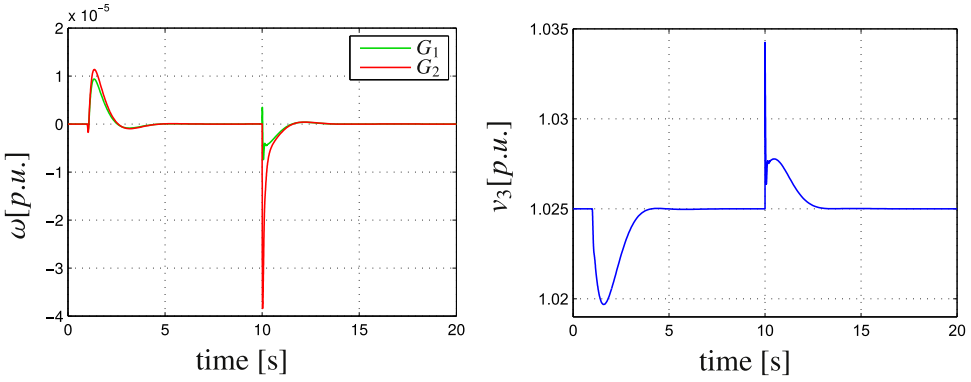

Fig. 12. Simulation of the SGs and WECS with LPV control, scenario 3.

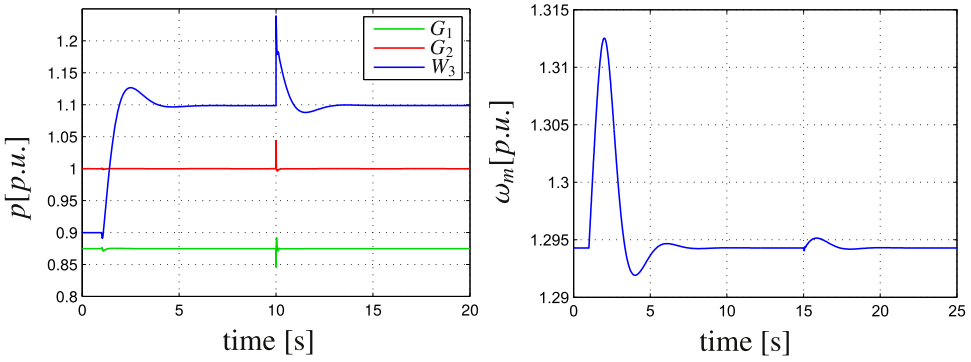

Fig. 13. Simulation of the injected powers and ω_m with LPV control, scenario 3.

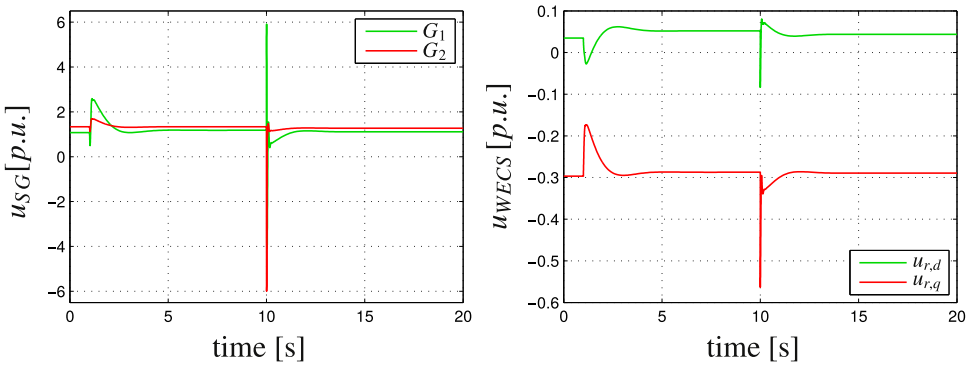

Fig. 14. Simulation results for the inputs with LPV control, scenario 3.

oscillations are visible for the voltage v_3 at bus 3. Although the generators still operate synchronously and the system remains stable, the oscillations have to be damped. Standard controllers are now introduced for all generators to contrast it to the proposed technique. Typically, a Power System Stabilizer (PSS) in combination with an Automatic Voltage Regulator (AVR) is used to achieve transient stability, to damp oscillations and to control the terminal voltage of the respective generator. The parameters are taken from (Shayeghi, Shayanfar, Jalilzadeh, & Safari, 2010) (same parametrization of the controllers for $G1$ and $G2$), and the simulation results for scenario 1 are shown in Fig. 4: the oscillations are damped down within 4 s and the voltage v_3 recovers to its initial value. In contrast, the oscillations of the LPV-controlled SGs vanish within 1 s, as can be seen for ω and v_3 in Fig. 5. The maximum amplitude of ω is half of the amplitude obtained for the case of control by the PSS-AVR scheme. In Fig. 6 the control actions of the two controller types are compared. While the amplitudes of the inputs of the standard controllers and the LPV-controlled G_1 and G_2 have amplitudes of less than 6 p.u., the amplitude of the LPV-controlled G_3 is significantly higher, leading to a better performance. To show the controller behavior and robustness for permanently changed operating conditions, the controllers are now tested for scenario 2. As it can be seen in Fig. 7, the oscillations of ω are damped down by the PSS-AVR, but they do not recover to a steady state. However, using the typical definition of transient stability, the system is still "stable" since the SGs are synchronous. The voltage is also damped, but cannot regain its original value. Usually, the original rotational velocity would be recovered by droop control, which is not in the focus of this work. However, by using the synthesis of LPV-controllers as proposed in this work, the grid returns to the original values of the rotational speeds of the SGs, as it can be seen in Fig. 8. At the same time, the voltage v_3 is controlled to its original value, showing that the LPV-controller of G_3 stabilizes the system and controls the voltage as well. The respective controller outputs of the standard and the LPV controllers can be seen in Fig. 9.

5.2. Control of the WECS

Now, the generator G_3 is replaced by the WECS W_3. With the initialization of $p_3 = 0.9$ (thus an amount of 90 MW of injected power), a reasonable interpretation is that W_3 represents a set of WECS. Thus, an aggregated model of several WECS is used, assuming that all WECS are subject to the same wind. The model from Section 2.2 and the parameters (in p.u.) remain valid. Only the power curve has to be scaled and interpreted as the sum of all wind turbines (Fernández et al., 2008). The power curve is chosen for the constant wind speed of $v_w = 11.4\frac{m}{s}$ and is shown in Fig. 2. The scenario in this section (scenario 3) is as follows: starting from steady state, the wind speed is changed from $v_w = 11.4\frac{m}{s}$ to $v_w = 12\frac{m}{s}$ at $t = 1$ s, and the line admittance between the buses 5 and 7 is doubled at $t = 10$ s, simulating a permanent change of the grid.

In Fig. 10, the results for the uncontrolled system with the SGs G_1, G_2 and the WECS W_3 are shown. After the wind changes, the angular velocities start to rise and finally become asynchronous after the line is switched. Similarly, unstable behavior can be observed in the course of the voltage v_3 at the point of connection of the WECS, which goes to zero by the end of the simulation.

In contrast to the system in Section 5.1, this system needs a controller to remain stable for the considered scenario. To address the controlled case, results with standard controllers are presented first. While G_1 and G_2 are controlled by PSS-AVR as described in the previous sub-section, the WECS is controlled by standard active and reactive power controllers. Their parameters and the exact structure can be found in Fernández et al. (2008). As it is shown in Fig. 11, the controllers manage to stabilize the system after the wind is changed, while the SGs do not recover to the original steady state value, but remain synchronous. At the same time, the voltage v_3 at the WECS almost completely recovers, showing steady state accuracy of the standard controller for the change of the wind. But when the operating point is changed at $t = 10$ s, the SGs do not remain synchronous any more, and the system becomes unstable.

Comparing this result to the LPV-controlled system, it can be seen in Fig. 12 that the LPV-controlled system remains stable during the whole simulation. The angular velocities of both SG return to their original values. The same applies for the voltage v_3, which is controlled by the WECS. The LPV-controlled system has a slightly larger drop after the wind changes, but it reaches its original value after 3 s. Overall, the system reacts robustly to changes of the wind and the grid, while quickly damping down the electromechanical oscillations. It can also be observed that the dynamics in response to the grid-changes is much faster than the dynamics caused by the wind. In Fig. 13, the steady state accuracy of the LPV-controller for ω_m and the respective injected power of W_3 (due to the higher wind speed) are shown. Finally, the inputs of the SGs and the WECS can be found in Fig. 14.

6. Conclusion

A unified modeling and synthesis technique is proposed and applied to grids comprising SGs and WECS. The resulting multi-objective LPV-controller ensures that both systems behave robustly for fluctuations caused either within the grid or are imposed by changing wind, and oscillations are well-damped. Using this technique for each of the nodes of a power grid ensures global stability, while the (decentralized) semi-definite programs for the local controller synthesis are of moderate size.

Future work will address the inclusion of photovoltaic (PV) systems into the multi-bus system. In fact, the applicability of the LPV-technique in the presence of the small time constants associated with the inverter of a PV-system showed positive results for a small instance of a grid in Theißen et al. (2016). Furthermore, in a closed system, the voltage control cannot be applied to all generating units, if the

generated power of the SG is constant. For that reason, the models of the SG and the control approach will be extended to balance the injected powers. This will allow a unified control approach for all three stability categories according to Kundur et al. (2004), i.e. stability of rotor angle, voltage, and frequency.

Acknowledgment

Partial financial support by the DFG through the project ROCS-Grid and by the EU through the H2020-project UnCoVerCPS (grant No. 643921) is gratefully acknowledged.

References

Anderson, P. M., & Fouad, A. A. (2003). *Power system control and stability* Piscataway, N.J.: Wiley-Interscience.

Apkarian, P., Gahinet, P., & Becker, G. (1995). Self-scheduled h_∞ control of linear parameter-varying systems: a design example. *Automatica*, *31*(9), 1251–1261.

Boyd, S. P., El Ghaoui, L., Feron, E., & Balakrishnan, V. (1994). *Linear matrix inequalities in system and control theory*, *15* Philadelphia, PA: SIAM.

Bünger, F. (2014). A note on the boundary shape of matrix polytope products. *Reliable Computing*, *20*, 73–88.

Chilali, M., & Gahinet, P. (1996). H_∞ design with pole placement constraints: an LMI approach. *IEEE Tr on Automatic Control*, *41*(3), 358–367.

Domínguez-García, J. L., Gomis-Bellmunt, O., Bianchi, F. D., & Sumper, A. (2012). Power oscillation damping supported by wind power: a review. *Renewable and Sustainable Energy Reviews*, *16*(7), 4994–5006.

Eremia, M. & Shahidehpour, M. (2013). *Handbook of electrical power system dynamics*: *modeling*, *stability, and control*, Vol. *92*, John Wiley & Sons, 2013.

Fan, L. (2009). Review of robust feedback control applic. in power systems. In *IEEE power systems conference*., pp. 1 –7.

Fernández, L. M., Jurado, F., & Saenz, J. R. (2008). Aggregated dynamic model for wind farms with doubly fed induction generator wind turbines. *Renewable Energy*, *33*(1), 129–140.

Fusco, G., & Russo, M. (2011). Nonlinear control design for excitation controller and power system stabilizer. *Control Eng Practice*, *19*(3), 243–251.

Gordon, M. & Hill, D. (2008). Global transient stability and voltage regulation for multimachine power systems. In *conversion and delivery of electrical energy in the 21st century*, pp. 1–8.

He, R., Liu K.-Z., Mei, S., & Gui, X. (2006). A gain-scheduled state feedback control method for transient stability control of a single-machine infinite-bus power system. In *Proceedings of the IEEE Chinese control conference* ., pp. 2147–2152.

He, R., Liu, K.-Z., & Mei, S. (2009). LPV modelling and gain-scheduled control approach for the transient stabilization of power systems. In *Proceedings of the 4th IEEE conference on Ind. electronics and applications* , pp. 29 –34.

Hughes, F. M., Anaya-Lara, O., Jenkins, N., & Strbac, G. (2006). A power system stabilizer for DFIG-based wind generation. *IEEE Tr on Power Systems*, *21*(2), 763–772.

Kundur, P. (1994). *Power system stability and control* New York: McGraw-Hill.

Kundur, P., Paserba, J., Ajjarapu, V., Andersson, G., Bose, A., Canizares, C., Hatziargyriou, N., Hill, D., Stankovic, A., Taylor, C., Van Cutsem, T., & Vittal, V. (2004). Definition and classification of power system stability, *IEEE Tr. D. on power systems 19* (2) 1387–1401.

Kwiatkowski, A., Boll, M.-T., & Werner, H. (2006). Automated generation and assessment of affine LPV models. *In Proceedings of the 45th IEEE conference on decision and control* , pp. 6690–6695.

Liu, H., Hu, Z., & Song, Y. (2012). Lyapunov-based decentralized excitation control for global asymptotic stability and voltage regulation of multi-machine power systems. *IEEE Tr on Power Systems*, *27*(4), 2262–2270.

Liu, Q., Vittal, V., & Elia, N. (2006). LPV supplementary damping controller design for a thyristor controlled series capacitor device. *IEEE Tr on Power Systems*, *21*(3), 1242–1249.

Liu, Q., Vittal, V., & Elia, N. (2006). Expansion of system operating range by an interpolated LPV FACTS controller using multiple Lyapunov functions. *IEEE Tr on Power Systems*, *21*(3), 1311–1320.

Miao, Z., Fan, L., Osborn, D., & Yuvarajan, S. (2009). Control of DFIG-based wind generation to improve interarea oscillation damping. *IEEE Tr on Energy Conversion*, *24*(2), 415–422.

Milano, F. (2010). *Power systems, Power system modelling and scripting* London, U.K.: Springer.

Mishra, Y., Mishra, S., Tripathy, M., Senroy, N., & Dong, Z. (2009). Improving stability of a DFIG-based wind power system with tuned damping controller. *IEEE Tr on Energy Conversion*, *24*(3), 650–660.

Mohammadpour, J., & Scherer, C. (2012). *Control of linear parameter varying systems with applications* Boston, MA: Springer.

Muhando, E. B., Senjyu, T., Uehara, A., & Funabashi, T. (2011). Gain-scheduled control for WECS via LMI techniques and parametrically dependent feedback part ii: controller design and implementation. *IEEE Tr on Industrial Electronics*, *58*(1), 57–65.

Qiu, W., Vittal, V., & Khammash, M. (2004). Decentralized power system stabilizer design using linear parameter varying approach. *IEEE Tr on Power Systems*, *19*(4), 1951–1960.

Rotondo, D., Nejjari, F., & Puig, V. (2013). A shifting pole placement approach for the design of parameter-scheduled state-feedback controllers. In *Proceedings of the European control conference*, pp. 1829–1834.

Schaab, K. & Stursberg, O. (2015). Decentralized robust control of power grids using LPV-models of DAE-systems. In 1^{st} *IFAC* workshop on linear-parameter-varying sys*tems*, pp. 418–423.

Schaab, K. & Stursberg, O. (2015). Robust decentralized LPV control for transient stability of power systems. In 9^{th} *IFAC symposium on control of power and energy systems*, pp. 566–571.

Shayeghi, H., Shayanfar, H., Jalilzadeh, S., & Safari, A. (2010). Multi-machine power system stabilizers design using chaotic optimization algorithm. *Energy Conversion and Management*, *51*(7), 1572–1580.

Theißen, M., Schaab, K., & Stursberg, O. (2016). Voltage stability of power grids with PV plants using robust LPV-control. In *control of transmission and distribution smart grids*.

Tóth, R. (2010). *Modeling and identification of linear parameter-varying systems*, *403* Berlin: Springer Science Business Media.

Wang, C., & Weiss, G. (2014). Linear parameter varying control of a doubly fed induction generator based wind turbine with primary grid frequency support. *International Journal of Robustness and Nonlinear Control*, *24*(14), 1927–1946.

Warren, J. (1996). Barycentric coordinates for convex polytopes. *Advances in Computational Mathematics*, *6*(1), 97–108.